Structural Characterization of a β-Diketone Hydrolase from the Cyanobacterium *Anabaena* sp. PCC 7120 in Native and Product-Bound Forms, a Coenzyme A-Independent Member of the Crotonase Suprafamily[†,‡]

Joseph P. Bennett, Jean L. Whittingham, A. Marek Brzozowski, Philip M. Leonard, and Gideon Grogan*

York Structural Biology Laboratory, Department of Chemistry, University of York, Heslington, York YO10 5YW, U.K.

Received September 13, 2006; Revised Manuscript Received October 19, 2006

ABSTRACT: The gene alr4455 from the well-studied cyanobacterium *Anabaena* sp. PCC 7120 encodes a crotonase orthologue that displays β-diketone hydrolase activity. *Anabaena* β-diketone hydrolase (ABDH), in common with 6-oxocamphor hydrolase (OCH) from *Rhodococcus* sp. NCIMB 9784, catalyzes the desymmetrization of bicyclo[2.2.2]octane-2,6-dione to yield [(*S*)-3-oxocyclohexyl]acetic acid, a reaction unusual among the crotonase superfamily as the substrate is not an acyl-CoA thioester. The structure of ABDH has been determined to a resolution of 1.5 Å in both native and ligand-bound forms. ABDH forms a hexamer similar to OCH and features one active site per enzyme monomer. The arrangement of side chains in the active site indicates that while the catalytic chemistry may be conserved in OCH orthologues, the structural determinants of substrate specificity are different. In the active site of ligand-bound forms that had been cocrystallized with the bicyclic diketone substrate bicyclo[2.2.2]octane-2,6-dione was found the product of the asymmetric enzymatic retro-Claisen reaction [(*S*)-3-oxocyclohexyl]acetic acid. The structures of ABDH in both native and ligand-bound forms reveal further details about structural variation and modes of coenzyme A-independent activity within the crotonases and provide further evidence of a wider suprafamily of enzymes that have recruited the crotonase fold for the catalysis of reactions other than those regularly attributed to canonical superfamily members.

The crotonase superfamily is a group of low sequence identity (typically <25%) proteins that catalyzes a wide range of different chemical reactions (*1*). The proteins exist, at one or other level of structural organization, as trimers or dimers of trimers, and despite the low sequence similarity, the overall fold of the monomer is well conserved between superfamily members (*2*). One key common feature of reactions catalyzed by crotonase superfamily members is the stabilization of enolate intermediates as part of the putative reaction coordinate (*1*). The enolate is stabilized by an oxyanion hole formed by the peptidic NHs of two residues and is conserved throughout the majority of known crotonases for which the structure has been determined. This conservation of intermediate stabilization facilitates the catalysis of, among others, the asymmetric hydration of carbon−carbon double bonds (by enoyl-CoA hydratase "crotonase") (*3*), the dehalogenation of chlorobenzene derivatives (4-chlorobenzoyl-CoA dehalogenase) (*4*), and the condensation of acetyl-coenzyme A (AcCoA) and glutamate semialdehyde to give (2*S*,5*S*)-carboxymethylproline in the biosynthesis of carbapenems (*5*). In all of these reactions, the substrate is an acyl-coenzyme A thioester derived from a carboxylic acid substrate via the action of a substrate-specific coenzyme A ligase. The varied and unexpected variety of chemical catalysis by crotonase superfamily members has had serious implications for the annotations of emerging genome sequences, as the function of these enzymes is difficult to predict from either sequence or genomic context alone (*6*).

As part of a study into novel enzyme-catalyzed desymmetrization processes, our attention had been drawn to the identification, by metabolite extraction and analysis, of a β-diketone hydrolase from *Rhodococcus* NCIMB 9784 that was able to catalyze the transformation, by apparent retro-Claisen reaction, of the bicyclic diketone 6-oxocamphor (**1**) to α-campholinic acid (**2**) (Figure 1) (*7*). In addition to studying the application of this enzyme as a preparative biocatalyst for the formation of chiral cyclic ketoacids, we isolated the enzyme, which we named 6-oxocamphor hydrolase (OCH),[1] and cloned and expressed in *Escherichia coli* the gene that encodes its activity (*8*). Gene sequencing revealed OCH to be a member of the crotonase superfamily but the first described for which the substrate was not an acyl-CoA thioester. The structure of OCH (*9*), and of a low k_{cat}/low K_M mutant that had the reaction product bound at the active site (*10*), confirmed the similarity of OCH to

[†] We thank the Biotechnology and Biosciences Research Council (BBSRC) for funding (Grant 87B/B17227) and for a studentship (to J.B.).

[‡] The atomic coordinates for the structure of native ABDH and of ABDH in complex with [(*S*)-3-oxocyclohexyl]acetic acid have been deposited in the Protein Data Bank as entries 2J5G and 2J5J, respectively.

* Corresponding author. Tel: 44 1904 328256. Fax: 44 1904 328266. E-mail: grogan@ysbl.york.ac.uk.

[1] Abbreviations: ABDH, *Anabaena* β-diketone hydrolase; OCH, 6-oxocamphor hydrolase; TLC, thin-layer chromatography; TMS, trimethylsilyl; MES, 2-(*N*-morpholino)ethanesulfonic acid; PEG, poly(ethylene glycol); SD, standard deviation.

10.1021/bi061900g CCC: $37.00
Published on Web 12/13/2006

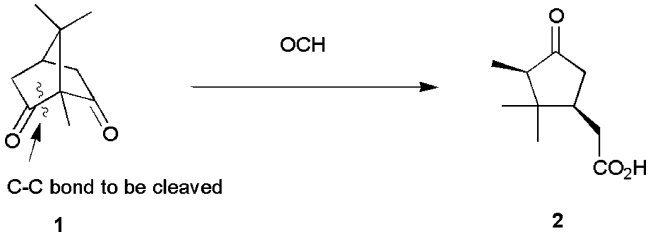

FIGURE 1: Desymmetrization by retro-Claisen reaction of 6-oxocamphor (**1**) to (2*R*,4*S*)-α-campholinic acid (**2**) by OCH from *Rhodococcus* sp. NCIMB 9784.

previously known crotonase structures and revealed molecular determinants of reactivity and selectivity that included both stabilization of an intermediate enolate in a noncanonical oxyanion hole for crotonases and a molecular basis for prochiral selectivity in the enzyme. This observation led us to suggest that OCH and related enzymes may form part of a wider crotonase *supra*family, in which the crotonase fold had been recruited for the catalysis of reactions with different mechanistic attributes to known crotonase enzymes (*10*).

While sequence-related variants of enoyl-CoA hydratase (crotonase) are abundant in sequenced genomes, there were, at the outset of this study, very few examples that suggested that the coenzyme A-independent crotonases displaying the retro-Claisenase activity of OCH were widely distributed. However, repeated BLAST searches of the SwissProt database revealed the presence of two closely sequence-related orthologues of OCH, encoded in the genomes of the cyanobacteria *Anabaena* PCC 7120 (*11*) and *Gloeobacter violaceous* PCC 7421 (*12*). The putative orthologue in *Anabaena*, corresponding to open reading frame alr4455 shared 46% sequence identity with OCH. Crucially, each of the acid−base residues that had been identified as perhaps having catalytic roles in OCH were conserved (His45, His122, His145, Asp154, and Glu243), and also the motif, largely conserved in crotonase enzymes, that contains one of the residues responsible for forming the oxyanion hole for stabilization of acyl-CoA thioesters (GGG or GAG), replaced in OCH by N(121)HP, was replaced in ABDH by L(120)HS (Figure 2). Examples of open reading frames that would encode equivalent putative active site residues have since been identified in the as-yet-incomplete genomes of *Xanthobacter* strain Py2 (Q26KU7**)**, *Frankia* EAN1pec (Q3W561), and *Mesorhizobium* sp. BNC1 (Q3WQH2) species (www. pedant.de).

The hydrolytic cleavage of carbon−carbon bonds continues to be a subject of substantial contemporary interest, as many of these processes have been demonstrated to have a crucial role in the biodegradation of aromatic compounds in the environment. C−C bond hydrolase activity had been identified in early microbiological studies of pathways in the degradation of gentisate, for example [fumarylpyruvate hydrolase (*13*, *14*), maleylpyruvate hydrolase (*13*)], and contemporary analytical and structural methods have allowed the dissection of the mechanism of a class of α,β-hydrolases active in the catabolism of phenylpropionate [2-hydroxy-6-ketonona-2,4-diene-1,9-dioic acid 5,6-hydrolase, MhPC (*15*)] and biphenyl [2-hydroxy-6-oxo-6-phenylhexa-2,4-dienoic acid hydrolase, BphD (*16*)]. The enzymatic cleavage of C−C bonds in β-diketones thus has growing significance for various aspects of bioremediation, biocatalysis, and mammalian physiology, and the mechanisms by which this particular cleavage is achieved are surprisingly diverse (*17*), ranging from metal-assisted hydrolytic processes (*18*) to those catalyzed by dioxygenases (*19*). As crotonases related to OCH were rare, and we were interested in discovering new activities that may have complementary selectivities to *Rhodococcus* OCH, we obtained the genomic DNA for *Anabaena* and cloned and expressed the gene encoding the *Anabaena* OCH orthologue, and we present herein our studies of the enzyme, which we have termed *Anabaena* β-diketone hydrolase (ABDH). We have found that ABDH from *Anabaena* does indeed catalyze the same retro-Claisenase reaction on a natural substrate analogue [bicyclo-[2.2.2]octane-2,6-dione (**3**), Figure 3] as OCH, but to a lesser degree, and the structure of the active site of the enzyme in complex with the product [[(*S*)-3-oxocyclohexyl]acetic acid (**4**)] reveals structural explanations for the observed activity.

EXPERIMENTAL PROCEDURES

Chemicals. Chemical reagents were purchased from Sigma and Aldrich. PCR primers were purchased from MWG Biotech. Restriction enzymes and corresponding buffers were purchased from New England Biolabs (NEB). LIC qualified T4 DNA polymerase (T4 pol) and KOD Hot Start DNA polymerase (KOD) were from Novagen; Pfu Turbo C_x Hot Start was from Stratagene. *E. coli* strains BL21-Gold (DE3) and XL-1 Blue were purchased from Stratagene and all others from Novagen. DNA purification kits were purchased from Qiagen. dNTPs were purchased from Bioline, and protein purification columns were from Amersham Life Sciences.

Gene Cloning, Expression, and Isolation of ABDH. The genomic DNA from *Anabaena* PCC 7120 was a generous gift from Professor Satoshi Tabata of the Kazusa DNA Institute, Chiba, Japan. The gene encoding the putative β-diketone hydrolase from *Anabaena* PCC 7120 was amplified by PCR using the primers (forward) CACCACCAC-CACATGATCTTGAATCAACCTGAATATTTCACC and (reverse) GAGGAGAAGGCGCGTTATTAAGTATTGCG-GAGATCG and was designed for insertion into the pETYS-BLIC vector (*20*). PCR reagents and conditions were as follows: template DNA (50 ng μL^{-1}), 0.5 μL; forward primer, 0.4 μM; reverse primer, 0.4 μM; 25 mM $MgSO_4$, 2 μL; 2 mM dNTP mix, 5 μL; KOD buffer, 5 μL; KOD, 1 μL; and sterile deionized water to a final volume of 50 μL. Following cleanup of the PCR product, a ligation-independent protocol, detailed in ref *20*, was used to clone the gene into plasmid pETYSBLIC, to create plasmid PL001, which would encode the protein of interest fused to a N-terminal hexahistidine tag. Sequencing confirmed the identity of the insert as alr4455. Soluble expression of the gene was achieved by inoculating a single colony into a 5 mL starter culture of Luria−Bertani broth and growing overnight at 37 °C. Fifty microliters of this starter was used to inoculate 500 mL of LB broth in a 2 L baffled Erlenmeyer flask. This culture was grown 37 °C in an orbital shaker at 150 rpm to an optical density (A_{500}) of 0.5, and 1 mM isopropyl thiogalactopyranoside (IPTG) was added to induce expression. The culture was then grown overnight at 16 °C, after which the cells were harvested by centrifugation. The combined cell pellets of four 0.5 L cultures were suspended in 100 mL of 50 mM HEPES buffer, pH 7.5, containing 20 μM phenylmethanesulfonyl fluoride and 300 mM sodium chloride (henceforth referred to as "the buffer"). The cell

```
ABDH          -MTLNQP--EYFTKYENLHFHRDENGILEVRMHTNGSSLVFTGKTHREFPDAFYDISRDR 57
OCH           MKQLATPFQEYSQKYENIRLERD-GGVLLVTVHTEGKSLVWTSTAHDELAYCFHDIACDR 59
                 *  *  **  ****:::.** .*:* * :**:*.***:*..:* *:. .*:**: **

ABDH          DNRVVILTGSGDAWMAEIDFPSLGDVTNPREWDKTYWEGKKVLQNLLDIEVPVISAVNGA 117
OCH           ENKVVILTGTGPSFCNEIDFTSF-NLGTPHDWDEIIFEGQRLLNN-LSIEVPVIAAVNGP 117
              :*:******:* ::  ****.*: :: .*::**:  :**:::*:* *.******:****.

ABDH          ALLHSEYILTTDIILASENTVFQDMPHLNAGIVPGDGVHILWPLALGLYRGRYFLFTQEK 177
OCH           VTNHPEIPVMSDIVLAAESATFQDGPHFPSGIVPGDGAHVVWPHVLGSNRGRYFLLTGQE 177
              .  *.*  : :**:**:*.:.*** **: :*******.*::** .**  ******:* ::

ABDH          LTAQQAYELNVVHEVLPQSKLMERAWEIARTLAKQPTLNLRYTRVALTQRLKRLVNEGIG 237
OCH           LDARTALDYGAVNEVLSEQELLPRAWELARGIAEKPLLARRYARKVLTRQLRRVMEADLS 237
              * *: * : ..*:***.:.:*: ****:** :*::* *  **:* .**::*:*::: .:.

ABDH          YGLALEGITATDLRNT--- 253
OCH           LGLAHEALAAIDLGMESEQ 256
               *** *.::* **
```

FIGURE 2: Sequence alignment of ABDH with OCH showing conservation of active site residues previously mutated in OCH and thought to contribute to catalysis in red (ABDH H43, H121, H144, D153, and E241). Residues in blue highlight the anticipated difference in active site topology between ABDH and OCH (vide infra). The conserved active site gate residues, F77 (ABDH), are highlighted in green.

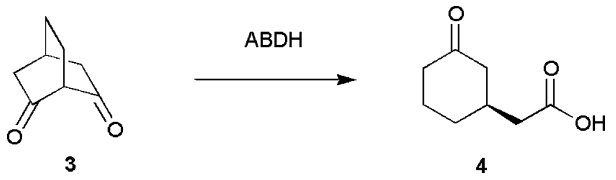

FIGURE 3: Reaction catalyzed by retro-Claisenase enzymes in this study. Both OCH and ABDH catalyze the retro-Claisen cleavage of bicyclo[2.2.2]octane-2,6-dione (**3**) to yield [(*S*)-3-oxocyclohexyl]-acetic acid (**4**).

suspension was subjected to sonication using three 30 s bursts with 1 min intervals. After disruption, the suspension was centrifuged and the supernantant filtered through a 0.2 μm filter (Amicon) in preparation for chromatography by FPLC. The filtered supernatant was loaded onto a nickel affinity HiTRAP agarose column and eluted using a gradient of 0−1 M imidazole in buffer. ABDH eluted in a large peak at a concentration of approximately 700 mM imidazole. Pooled fractions containing ABDH as confirmed by SDS−PAGE were then applied in 5 mL aliquots to an S200 16/60 Sephadex column (Pharmacia) and eluted with the buffer. Recovered ABDH was maintained at concentration of 1 mg mL^{-1} as determined by A_{280} ultraviolet spectrophotometry measurements using a Biophotometer (Eppendorf) and corrected using a theoretical molar extinction coefficient of 42400 mol^{-1} dm^3 cm^{-1} as calculated using the EXPASY molecular biology server (http://ca.expasy.org/).

Enzyme Assays. The retro-Claisenase activity of OCH and ABDH was quantified using bicyclo[2.2.2]octane-2,6-dione as substrate, which was synthesized as described previously (*7*). Typically, a solution of the substrate at the required concentration was made up in 50 mM HEPES buffer, pH 7.0, and to this was added enzyme from a concentrated solution to a final concentration of ~0.1 mg mL^{-1}. The disappearance of substrate was monitored spectrophotometrically at 285 nm, using a molecular extinction coefficient for the substrate of 122.5 mol^{-1} dm^3 cm^{-1}. Kinetic parameters were determined from the results of experiments using substrate concentrations of 0.1, 0.25, 0.5, 1.0, 1.5, 2.0, 2.5, 3.0, 4.0, 5.0, 7.5, and 10 mmol dm^{-3}.

Biotransformations of bicyclo[2.2.2]octane-2,6-dione were performed as described previously, for both OCH and ABDH (*7*). When reactions were complete, as determined by the apparent disappearance of substrate by TLC, the mixture was acidified to pH 4, and the mixture was extracted with ethyl acetate. The organic fraction was dried using anhydrous magnesium sulfate, and after the solvent was removed, the crude keto acid products were converted to their methyl esters using TMS-diazomethane (*21*). A racemic standard of the appropriate methyl ester was prepared by methanolysis of the substrate using the procedure described previously (*7*). Chiral GC analysis of the methyl ester products was performed on an Agilent 6890 gas chromatograph fitted with an Agilent Cyclosil B column (inlet temperature 250 °C, detector temperature 320 °C); a gradient of 100−200 °C at a rate of 3 °C min^{-1} was used to separate the enantiomers of (3-oxocyclohexyl)acetic acid methyl ester which eluted at 24.3 (*R*) and 24.5 (*S*) min.

Crystallization. Initial crystallization conditions were obtained from the "clear strategy screen" (*22*) using the sitting drop method of vapor diffusion with 150 nL of protein plus 150 nL of precipitant solution drops in a 96-well plate using a Mosquito liquid handling robot. Scale-up of successful conditions was effected using 1 μL plus 1 μL hanging drops in a 24-well Linbro dish. ABDH solution used routinely for crystallization was at a concentration of 10 mg mL^{-1} in the buffer. The conditions and solutions for cryogenic protection for the three structures presented in this report were as follows: for ABDH native, 100 mM MES, pH 5.5, 15% (w/v) PEG 4000, and 0.8 mol dm^{-3} sodium formate (crystals were frozen in a cryoprotectant solution of the same components plus 15% hexanetriol); for ABDH complexed with [(*S*)-3-oxocyclohexyl]acetic acid, 100 mM bis-tris propane, pH 7.5, 20% (w/v) PEG 3350, 0.2 mol dm^{-3} sodium malonate, and 10 mM bicyclo[2.2.2]octane-2,6-dione [crystals were frozen in a cryoprotectant solution of the same components plus 20% (v/v) hexanetriol].

Data Collection. Data were collected at the European Synchrotron Radiation Facility (ESRF), Grenoble, France, during 2005/6. Details of data collection and refinement statistics for the three structures described herein are presented in Table 1.

Structure Solution. (1) Structure Solution of Native ABDH. The native structure of ABDH was indexed in the space group $P2_1$, with the Matthews coefficient (*23*) suggesting the asymmetric unit contained 12 monomers. The structure

Table 1: Data Collection and Refinement Statistics for ABDH and Ligand Complexes[a]

	ABDH	
	native	complex with **4**
beamline	ID14	ID23
wavelength (Å)	0.93	1.07
resolution (Å)	50.00−1.46 (1.51−1.46)	40.19−1.57 (1.63−1.57)
space group	$P2_1$	$P6_3$
unit cell (Å)	118.00, 83.19, 154.01	80.39, 80.39, 125.88
unique reflections	515541	64435
completeness (%)	97.7 (86.8)	98.9 (89.9)
R_{sym} (%)	6.7 (27.0)	6.4 (27.4)
multiplicity	4.4 (3.4)	10.1 (4.8)
$\langle I/\sigma(I)\rangle$	22.3 (4.7)	32.0 (2.9)
protein atoms	24295	4180
solvent waters	4421	714
R_{cryst}	0.157	0.145
R_{free}	0.180	0.171
rmsd 1−2 bonds (Å)	0.014 [0.022]	0.014 [0.022]
rmsd 1−3 angles (deg)	1.5 [2.0]	1.5 [2.0]
chiral center (Å^3)	0.102 [0.200]	0.106 [0.200]
planarity	0.009 [0.020]	0.008 [0.020]
av main chain B (Å^2)	10	12
av side chain B (Å^2)	12	14
av solvent B (Å^2)	27	25

[a] Values in parentheses refer to the highest resolution shell. Values in square brackets are target values. $R_{sym} = \sum_h\sum_l|I_{hl} - \langle I_h\rangle|/\sum_h\sum_l\langle I_h\rangle$, where I_l is the lth observation of reflection h and $\langle I_h\rangle$ is the weighted average intensity for all observations l of reflection h. $\langle I/\sigma(I)\rangle$ indicates the average of the intensity divided by its average SD.

of 6-oxocamphor hydrolase (OCH, 46% sequence identity, 1o8u) was used as an initial model for molecular replacement trials with MOLREP (*24*). Using an OCH monomer as a search model, MOLREP (*24*) gave a correct solution of the 12 monomers arranged as double hexamers. Subsequent refinement by REFMAC (*25*) gave an initial *R* factor of 0.24 and R_{free} of 0.26. The structure of ABDH cocrystallized with bicyclo[2.2.2]octane-2,6-dione was indexed in the space group $P6_3$, a space group not common for members of the crotonase superfamily. Interestingly, the Matthews coefficient suggested that only 2 monomer units were in the asymmetric unit, and this was confirmed after molecular replacement with MOLREP (*24*), using a monomer of the already solved native ABDH. The highest scoring molecular replacement solution was correct, and subsequent refinement by REFMAC gave an *R* factor of 0.22 and R_{free} of 0.26.

Model Building and Refinement. For each of the structures, 5% of the total reflections were flagged for cross-validation before refinement. These data were used to monitor the modeling process at various stages of refinement for the weighting of geometrical and temperature factor restraints. All computing was undertaken by the CCP4 suite (*26*). The model building and refinement were carried out with REFMAC in conjunction with ARP/wARP (*27*) in the resolution ranges listed in Table 1. Coot (*28*) was used for manual corrections to the models.

(1) Model Building and Refinement of Native ABDH. The N-termini were visible in electron density maps from Asn4/Gln5. The C-termini were modeled to Asn252/Thr253, Thr253 being the final residue in the sequence. A total of 3706 water molecules were modeled via a combination of ARP/wARP and manual methods using Coot. In addition to solvent molecules, the density for sulfate (SO_4^{2-}) ions was observed at each trimer interface, and these were modeled in also using Coot. Analysis of Ramachandran plots indicated that 93.6% of the residues were in the most favored regions, 6.4% in additionally allowed regions, and none in generously allowed regions, as indicated by PROCHECK (*29*).

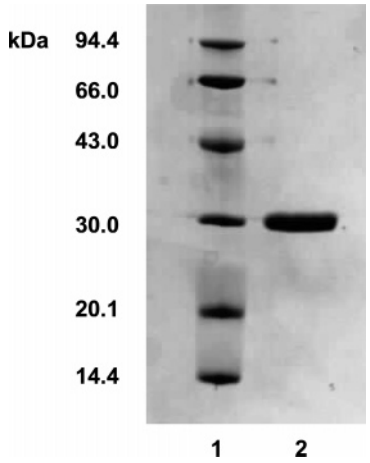

FIGURE 4: SDS−PAGE of pure ABDH from *Anabaena* PCC 7120 after nickel affinity chromatography and gel filtration. The enzyme has a subunit molecular mass of approximately 30 kDa, in agreement with the predicted value of 28.8 kDa. Lane 1: low MW markers (Bioline). Lane 2: ABDH from *Anabaena* PCC 7120 expressed in *E. coli* BL21(DE3).

(2) Model Building and Refinement of ABDH Bound to [(S)-3-Oxocyclohexyl]acetic Acid. The N-termini were visible in electron density maps from Thr2/Gln5. The C-termini were modeled up to Asn252/Thr253. A total of 714 water molecules were identified. Electron density maps indicated density in each active site corresponding to the expected product of C−C bond cleavage, [(*S*)-3-oxocyclohexyl]acetic acid (**4**). Coordinate files and bond angle/distance data for this ligand were generated using the PRODRG server (*30*). At the theoretical trimer interface (taking into account symmetry-related molecules) additional density was observed. Anomalous difference maps generated by Coot strongly suggest that this density was a metal ion. Further refinement led to the identification of the metal as Ni^{2+}. Analysis of Ramachandran plots indicated that 93.7% of the residues were in the most favored regions, 6.3% in additionally allowed regions, and none in generously allowed regions, as indicated by PROCHECK (*29*).

RESULTS

(1) Isolation and Characterization of ABDH. An SDS−PAGE gel showing the pure ABDH is shown in Figure 4. ABDH exhibited the expected molecular mass of approximately 30 kDa, and calibrated gel filtration suggested that the physiological quaternary structure was a hexamer (data not shown). A selection of commercially and locally available diketone substrates including cyclohexane-1,3-dione, benzoylacetone, 2-acetylcyclohexanone, bicyclo[3.3.0]-octane-2,8-dione, 2,4-pentanedione, and 2,2,dimethylcyclohexane-1,3-dione were not transformed by ABDH (data not shown), although, in common with OCH, bicyclic, nonenolizable β-diketones proved to be substrates. The ability of ABDH to catalyze the retro-Claisen cleavage of bicyclo-[2.2.2]octane-2,6-dione was assessed using a spectrophotometric assay based on the disappearance of substrate and

Table 2: Kinetic Constants for OCH and ABDH in the Catalysis of Retro-Claisen Cleavage of **3**

enzyme	k_{cat} (s^{-1})	K_M (mol dm^{-3})	k_{cat}/K_M (s^{-1} mol^{-1} dm^3)
OCH	0.75	7.9×10^{-4}	9.5×10^2
ABDH	0.16	4.4×10^{-3}	0.36×10^2

was compared to results obtained for OCH using the same substrate. k_{cat}/K_M values were obtained in each case (Table 2), and values of 9.5×10^2 and 0.36×10^2 s^{-1} mol^{-1} dm^3 were recorded for OCH and ABDH, respectively. OCH activity with the synthetic substrate bicyclo[2.2.2]octane-2,6-dione was markedly reduced by 10^5 compared to that observed for the natural substrate, 6-oxocamphor (*8*), which has k_{cat}/K_M of 1.61×10^7 s^{-1} mol^{-1} dm^3. While these results suggest that ABDH is an even poorer catalyst for the transformation of the synthetic substrate, prochiral selectivity exhibited by OCH for the transformation was conserved, ABDH yielding the (*S*)-keto acid (as determined by chiral GC analysis of the corresponding methyl ester) with 84% enantiomeric excess.

(2) Structure of Native ABDH. The structure of native ABDH was solved to a resolution of 1.46 Å (Figure 5). The asymmetric unit contained 12 monomers [(A)−(L)] arranged in two hexamers that are a common quaternary state observed in members of the crotonase superfamily. Unsurprisingly, given the close sequence identity between OCH and ABDH, the ABDH monomer (Figure 6) is of the "self-associating" fold as described by Hubbard and co-workers (*31*). The rmsd for the overlap of Cα atoms for the whole monomer was 0.82 Å. Each trimer interface contained what appears to be a sulfate ion (SO_4^{2-}), presumably sequestered from the affinity purification step. In each case, this ion was coordinated to the terminal amino groups of Arg230 from the three monomers making up the relevant trimer. In a similar fashion, the sulfate ion was also coordinated to N(E) of Arg227 of each monomer in the trimer. Other intertrimer stabilizing interactions include hydrogen bonds between the phenolic hydroxyl of Tyr170 (A) and Glu191 (C), Tyr166 (A), and the backbone carbonyl of Leu126 (C) and Leu224 (A) in a hydrophobic interaction with Leu172 (C). Various intratrimer interactions were also observed. The terminal NH of Gln101 (A) hydrogen bonds to the hydroxyl group of Asp105 (D), the terminal NH of Lys97 (A) hydrogen bonds to the hydroxyl group of Glu107 (D), Tyr219 (A) forms a π-stacking interaction with Tyr93 (D), as do Tyr51 (A) and Tyr51 (D). The phenolic hydroxyl of Tyr51 also forms a hydrogen-bonding interaction with the side chain amide of Asn102 (D), as do the hydroxyl group of Asp48 (A) and the terminal amino group of Arg55 (D) (∼2.9 Å). A further feature of note was the position of Phe77, mooted to act as a "gate" to the active site cavity in OCH. In the case of the native structure, this appears to be in the "open" conformation, allowing access to the active site.

(3) Structure of ABDH Bound to [(S)-3-Oxocyclohexyl]-acetic Acid. In an attempt to obtain a crystal structure of ABDH with a ligand bound in the active site, the protein was cocrystallized with the substrate bicyclo[2.2.2]octane-2,6-dione (**3**). The structure of ABDH in complex with the product of retro-Claisen cleavage of the substrate, [(*S*)-3-oxocyclohexyl]acetic acid (**4**), was solved to a resolution of 1.57 Å. While the global structure was almost identical to that of the native structure (all inter- and intratrimer interactions previously mentioned being conserved and observed with symmetry-related molecules), it was interesting to note a nickel center in the trimer interface, which had presumably resulted from nickel sequestered during affinity chromatography. The nickel ion in each case appeared to be coordinated to five water molecules. Figure 7 shows the result of this cocrystallization experiment, wherein the density of [(*S*)-3-oxocyclohexyl]acetic acid (**4**), the product of enzymatic reaction confirmed by biotransformation and chiral GC assay (vide supra), was clearly visible. The carboxylate of the product was strongly hydrogen bonded to a water molecule that is bound to His144 and also associated with His121 and His43. The carbonyl group of the cyclohexanone ring was not hydrogen bonded to active site residues, although the cyclohexanone ring is sandwiched between Leu80, Ile149, and Val83. There appeared to be little change in active site side chain orientation as a result of substrate binding, although the highly mobile gate Phe77 (*B* factor 18.75, occupancy 0.5) has shifted with respect to the native structure and appears to be in a "closed" position over the active site cavity. Another notable feature was the movement of residue Leu80 with respect to the same residue in the native ABDH structure. In monomer A, Leu80 has swiveled 90° away from the bound [(*S*)-3-oxocyclohexyl]acetic acid (**4**) at the Cδ position. Interestingly, in the native ABDH Leu80 is in the same position as its respective residue in OCH (Phe82), pointing toward the active site. It seems that Leu80 has moved to accommodate the [(*S*)-3-oxocyclohexyl]-acetic acid (**4**) molecule in that particular orientation in the active site.

DISCUSSION

Anabaena sp. (*Nostoc*) PCC 7120 has assumed significance in microbiological research as a model for mechanisms of prokaryotic photosynthesis, and several crystal structures of proteins (notably those involved in redox biochemistry) from the organism have been the focus of interest (*32*). *Anabaena* is also of interest being a member of that class of cyanobacteria that causes the fouling of water through the production of alkaloids such as anatoxin (*33*) and terpenes such as methylisoborneol (1-*exo*-hydroxy-2,3,3-trimethylbicyclo[2.2.1]heptanol) (*34*). The latter characteristic is perhaps most relevant in the context of this report, as it reveals the capacity of *Anabaena* to undertake terpene metabolism of structures very closely related to camphor (2,3,3-trimethylbicyclo[2.2.1]heptanone). The sequence of alr4455 shares only 46% identity with OCH, and hence it is difficult to be certain of assigning reaction specificity to the putative gene product, and indeed, the genomic context of alr4455 is unrevealing, the only proximal sequence of note being a tropinone reductase adjacent to alr4455 on the genome. However, it was the specific conservation of five active site acid/base residues (His43, His121, His144, Asp154, and Glu243) from OCH to ABDH that informed the choice of ABDH as a possible target in searching for homologues of OCH that may possess altered selectivity. It was noted that although residues that had been identified as contributing to acid−base catalysis in the mechanism of OCH were conserved, other active site residues that were involved in substrate binding and intermediate stabilization were not. Notable among these were Phe38 (for Trp40) and Leu80 (for

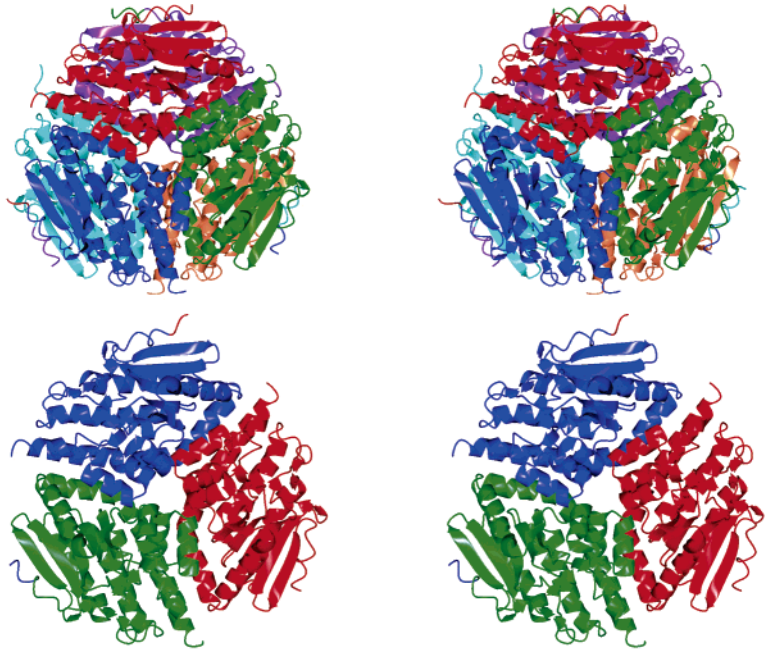

FIGURE 5: Stereoviews of trimeric (top) and hexameric (bottom) substructures of ABDH. Each monomer contains one active site.

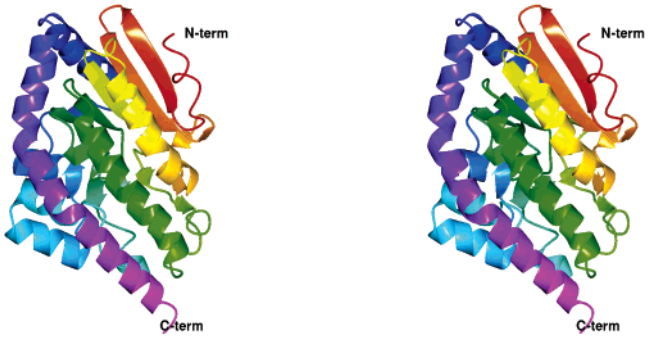

FIGURE 6: Stereoview of the structure of the monomer of ABDH (N-terminal, red; C-terminal, magenta) displaying a β-α-β superhelix fold common among crotonase enzymes. The C-terminal helix loops around the N-terminal domain, describing the self-association crotonase fold as defined by Hubbard and co-workers (*31*).

Phe82), which had been shown to comprise part of the oxyanion hole for enolate stabilization in the reaction coordinate of OCH catalysis and the primary determinant of prochiral selectivity in OCH, respectively.

As a result of the significant anticipated differences in active site topology between the two enzymes, it was thought that ABDH may display different selectivity to that observed for OCH. However, investigation suggests that the *pro-S* selectivity of OCH is conserved. That the enantiomeric excess was slightly lower for ABDH than OCH may be attributed either to a lower inherent selectivity of the enzyme for the substrate due to greater mobility in the active site or, more likely, because of residual substrate in the spent enzyme reaction being nonselectively hydrolyzed during workup. However, a significant difference in the activity of ABDH compared to OCH was recorded. Although k_{cat}/K_M for OCH when using the natural substrate analogue bicyclo[2.2.2]-octane-2,6-dione (**3**) was greatly reduced compared to 6-oxocamphor (**1**), OCH proved to be an effective catalyst for the desymmetrization of the substrate. The reasons for the poor catalytic activity of ABDH with the synthetic substrate might be predicted from the sequence, given that the tryptophan residue (Trp40) that is at least partially responsible for binding one of the substrate carbonyl groups in OCH (*10*) is absent in ABDH and that the phenylalanine (Phe82), which was thought to confer some measure of stereochemical control in OCH, was replaced by a leucine residue (Leu80).

These interactions between the enzyme active site and ligand are illuminated by the structure of ABDH in the presence of [(*S*)-3-oxocyclohexyl]acetic acid (**4**), which provides the first structure of a wild-type coenzyme A-independent crotonase enzyme with a bound ligand. If the structure is compared to the His122Ala mutant of OCH bound to its reaction product, a number of differences become clear. The cycloalkanone ring of the product is not stacked against a phenylalanine ring as for OCH but has shifted to be accommodated between two hydrophobic residues below the catalytic residues in the active site. In addition, the structure appears to represent a distance further along from the OCH mutant structure in terms of reaction coordinate: the keto acid product has relaxed into a flat conformation, the keto acid carboxylate is bound now by His121 and not Glu243, and a water molecule is clearly observed between the carboxylate oxygen and His144, suggesting preparation for the next catalytic turnover on product release. The degree of overlap between His144(145), Asp153(154), and the gate residue Phe77(89) is pronounced, again indicative of conservation of function of these residues between orthologues. Figure 8 summarizes the differences and similarities in active site topology between OCH and ABDH. The overlap of ligand-bound active sites suggests that while conservation of catalytic residues, on the left-hand side of the active site as shown, implies conservation of catalytic function by ABDH, the natural substrate specificity, as determined by other areas of the active site, is almost certainly different. A summary of the proposed mechanism of C−C bond cleavage by ABDH, based on results obtained for both OCH (*10*) and the results described herein, is shown in Figure 9.

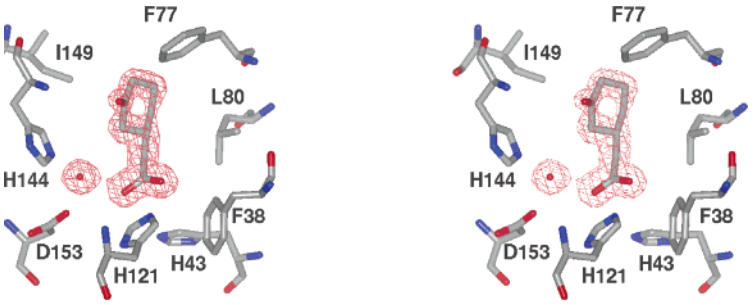

FIGURE 7: Active site of ABDH complexed with [(*S*)-3-oxocyclohexyl]acetic acid. Ligand electron density corresponds to the $2F_o - 2F_c$ electron density map contoured at the 1σ level. The carboxylate of the ligand can be seen hydrogen bonded to a water molecule, which is in turn bonded to the catalytic base residue His144, which is thought to activate a water molecule for attack at the substrate *pro-S* carbonyl in OCH. This is perhaps representative of the product leaving the active site prior to the next catalytic turnover.

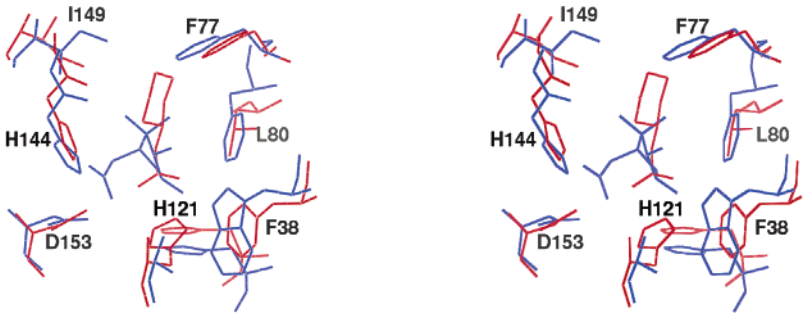

FIGURE 8: Overlap of active site residues and ligands for the OCH His122Ala mutant bound to α-campholinic acid (red) and ABDH bound to [(*S*)-3-oxocyclohexyl]acetic acid (blue). While the catalytic chemistry is conserved, e.g., OCH His145/ABDH His144, all substrate binding residues are not (e.g., OCH Trp40 replaced by Phe38; OCH Phe82 replaced by ABDH Leu80).

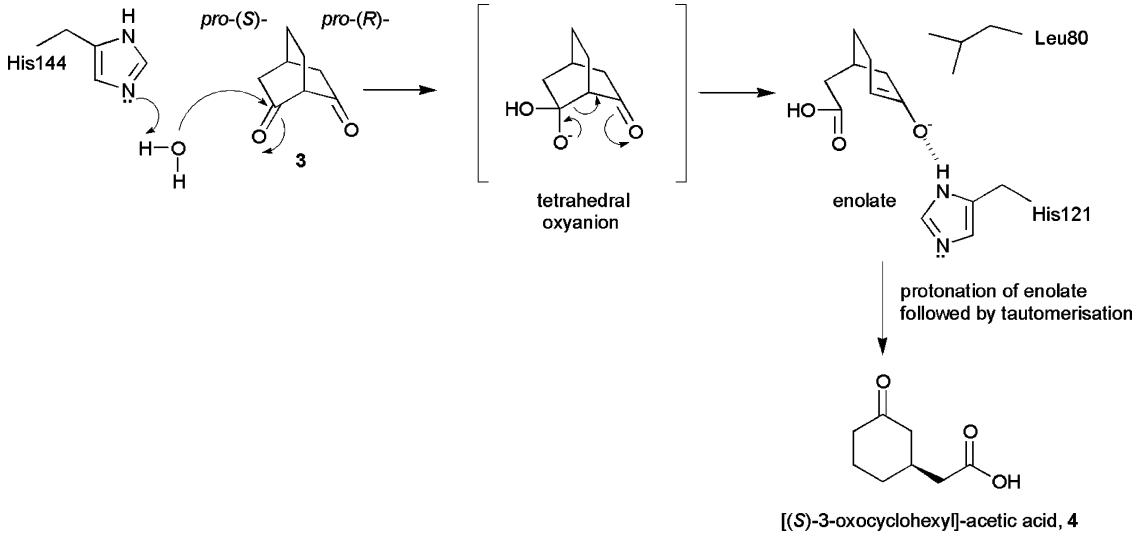

FIGURE 9: Mechanism proposed for ABDH-catalyzed carbon−carbon bond cleavage. Base-catalyzed activation of a water molecule by His144 at the *pro-S* face of substrate **3** results in a tetrahedral oxyanion, which rearranges to form an enolate intermediate that is stabilized by His121. Protonation and subsequent tautomerization give rise to the single enantiomer keto acid product **4**.

In summary, we have identified, by genome mining, an orthologue of a retro-Claisenase from *Rhodococcus* sp. in the cyanobacterium *Anabaena* PCC 7120. Studies of the enzyme using biotransformation and structural techniques have revealed an additional rare example of an orthologue among the crotonase-related enzymes that is not dependent on the ligation of its substrate to coenzyme A for substrate recognition. As such, the structure and demonstrable activity of ABDH serve to illustrate the wider distribution of a functional OCH-like family within a crotonase suprafamily as defined by Gerlt and Babbitt (*6*) and provide further information on substrate binding modes in cyanobacterial crotonase orthologues, which are a subject of current interest in the area of polyketide biosynthesis (*35*). OCH and ABDH are examples of crotonase enzymes that do not fulfill the criteria previously associated with membership of a crotonase superfamily and further reflect the scope of natural evolution to generate a surprising breadth of catalytic diversity within one protein fold. Such observations of natural enzyme evolution may help to inform both rational and random design of novel enzyme activities in the future. We are currently using available databases to explore the existence and activity of other noncanonical crotonase orthologues with unusual enzyme activities.

ACKNOWLEDGMENT

We thank Professor Satoshi Tabata of the Kazusa DNA Institute, Japan, for the gift of *Anabaena* PCC 7120 genomic DNA.

REFERENCES

1. Holden, H. M., Benning, M. M., Haller, T., and Gerlt, J. A. (2001) The crotonase superfamily: divergently related enzymes that catalyze different reactions involving acyl coenzyme A thioesters, *Acc. Chem. Res. 34*, 145−157.
2. Hubbard, P. A., Yu, W., Sculz, H., and Kim, J.-J. P (2005) Domain swapping in the low-similarity isomerase/hydratase superfamily: the crystal structure of rat mitochondrial Δ^3, Δ^2-enoyl-CoA isomerase, *Protein Sci. 14*, 1545−1555.
3. Engel, C. K., Mathieu, M., Zeelen, J. Ph., Hiltunen, J. K., and Wierenga, R. K. (1996) Crystal structure of enoyl-coenzyme A (CoA) hydratase at 2.5 Ångstroms resolution: a spiral fold defines the CoA-binding pocket, *EMBO J. 15*, 5135−5145.
4. Benning, M. M., Taylor, K. L., Liu, R.-Q., Yang, G., Xiang, H., Wesenberg, G., Dunaway-Mariano, D., and Holden, H. M. (1996) Structure of 4-chlorobenzoyl coenzyme A dehalogenase determined to 1.8 Å resolution: an enzyme catalyst generated via adaptive mutation, *Biochemistry 35*, 8103−8109.
5. Sleeman, M. C., and Schofield, C. J. (2004) Carboxymethylproline synthase (CarB), an unusual carbon-carbon bond-forming enzyme of the crotonase superfamily involved in carbapenem biosynthesis, *J. Biol. Chem. 279*, 6730−6736.
6. Gerlt, J. A., and Babbitt, P. C. (2001) Divergent evolution of enzyme function: mechanistically diverse superfamilies and functionally distinct suprafamilies, *Annu. Rev. Biochem. 70*, 209−246.
7. Grogan, G., Graf, J., Jones, A., Parsons, S., Turner, N. J., and Flitsch, S. L. (2001) An asymmetric enzyme-catalyzed retro-Claisen reaction for the desymmetrisation of cyclic beta-diketones, *Angew. Chem., Int. Ed. Engl. 40*, 1111−1114.
8. Grogan, G., Roberts, G. A., Bougioukou, D., Turner, N. J., and Flitsch, S. L. (2001) The desymmetrization of bicyclic β-diketones by an enzymatic retro-Claisen reaction, a new reaction of the crotonase superfamily, *J. Biol. Chem. 276*, 12565−12572.
9. Whittingham, J. L., Turkenburg, J. P., Verma, C. S., Walsh, M. A., and Grogan, G. (2003) The 2-Å crystal structure of 6-oxo camphor hydrolase. New structural diversity in the crotonase superfamily, *J. Biol. Chem. 278*, 1744−1750.
10. Leonard, P. M., and Grogan, G. (2004) Structure of 6-oxo camphor hydrolase H122A mutant bound to its natural product, (2S,4S)-α-campholinic acid. Mutant structure suggests an atypical mode of transition state binding for a crotonase homolog, *J. Biol. Chem. 279*, 31312−31317.
11. Kaneko, T., Nakamura, Y., Wolk, C. P., Kuritz, T., Sasamoto, S., Watanabe, A., Iriguchi, M., Ishikawa, A., Kawashima, K., Kimura, T., Kishida, Y., Kohara, M., Matsumoto, M., Matsuno, A., Muraki, A., Nakazaki, N., Shimpo, S., Sugimoto, M., Takazawa, M., Yamada, M., Yasuda, M., and Tabata, S. (2001) Complete genomic sequence of the filamentous nitrogen-fixing cyanobacterium *Anabaena* sp. strain PCC 7120, *DNA Res. 8*, 205−213.
12. Nakamura, Y., Kaneko, T., Sato, S., Mimuro, M., Miyashita, H., Tsuchiya, T., Sasamoto, S., Watanabe, A., Kawashima, K., Kishida, Y., Kiyokawa, C., Kohara, M., Matsumoto, M., Matsuno, A., Nakazaki, N., Shimpo, S., Takeuchi, C., Yamada, M., and Tabata, S. (2003) Complete genome structure of *Gloeobacter violaceus* PCC 7421, a cyanobacterium that lacks thylakoids, *DNA Res. 10*, 137−145.
13. Bayly, R. C., Chapman, P. J., Dagley, S., and Berardino, D. D. (1980) Purification and some properties of maleylpyruvate and fumarylpyruvate hydrolase from *Pseudomonas alcaligines*, *J. Bacteriol. 143*, 70−77.
14. Zhou, N.-Y., Fuenmayor, S. L., and Williams, P. A. (2001) *nag* genes of *Ralstonia* (formerly *Pseudomonas*) sp. strain U2 encoding enzymes for gentisate catabolism, *J. Bacteriol. 183*, 700−708.
15. Dunn, G., Montgomery, M. G., Mohammed, F., Coker, A., Cooper, J. B., Robertson, T., Garcia, J. L., Bugg, T. D. H., and Wood, S. P. (2005) The Structure of the C-C bond hydrolase MhpC provides insights into the catalytic mechanism, *J. Mol. Biol. 346*, 253−265.
16. Horsman, G. P., Ke, J. Y., Dai, S. D., Seah, S. Y. K., Bolin, J. T., and Eltis, L. D. (2006) Kinetic and structural insight into the mechanism of BphD, a C-C bond hydrolase from the biphenyl degradation pathway, *Biochemistry 45*, 11071−11086.
17. Grogan, G. (2005) Emergent mechanistic diversity of enzyme-catalysed β-diketone cleavage, *Biochem. J. 388*, 721−730.
18. Bateman, R. L., Bhanumoorthy, P., Witte, J. F., McClard, R. W., Grompe, M., and Timm, D. E. (2001) Mechanistic inferences from the crystal structure of fumarylacetoacetate hydrolase with a bound phosphorus-based inhibitor, *J. Biol. Chem. 276*, 15284−15291.
19. Straganz, G. D., Hofer, H., Steiner, W., and Nidetzky, B. (2004) Electronic substituent effects on the cleavage specificity of a non-heme Fe^{2+}-dependent beta-diketone dioxygenase and their mechanistic implications, *J. Am. Chem. Soc. 126*, 12202−12203.
20. Bonsor, D., Butz, S. F., Solomons, J., Grant, S. C., Fairlamb, I. J. S., Fogg, M. J., and Grogan, G. (2006) Ligation independent cloning (LIC) as a rapid route to families of recombinant biocatalysts from sequenced prokaryotic genomes, *Org. Biomol. Chem. 4*, 1252−1260.
21. Presser, A., Huefner, A., and Singer, D. (2004) Trimethylsilyldiazomethane—a mild and efficient reagent for the methylation of carboxylic acids and alcohols in natural products, *Monatsh. Chem. 138*, 1015−1022.
22. Brzozowski, A. M., and Walton, J. (2000) Clear strategy screens for macromolecular crystallization, *J. Appl. Crystallogr. 34*, 97−101.
23. Matthews, B. W. (1968) Solvent content of protein crystals, *J. Mol. Biol. 33*, 491−497.
24. Vagin, A., and Teplyakov, A. (1997) MOLREP: an automated program for molecular replacement, *J. Appl. Crystallogr. 30*, 1022−1025.
25. Murshudov, G. N., Vagin, A. A., and Dodson, E. J. (1997) Refinement of macromolecular structures by the maximum-likelihood method, *Acta Crystallogr., Sect. D: Biol. Crystallogr. 53*, 240−255.
26. Collaborative Computational Project, Number 4 (1994) *Acta Crystallogr., Sect. D: Biol. Crystallogr. 50*, 760−763.
27. Perrakis, A., Morris, R., and Lamzin, V. S. (1999) Automated protein model building combined with iterative structure refinement, *Nat. Struct. Biol. 6*, 458−463.
28. Emsley, P., and Cowtan, K. (2004) Coot: model-building tools for molecular graphics, *Acta Crystallogr., Sect. D: Biol. Crystallogr. 60*, 2126−2132.
29. Laskowski, R. A., Macarthur, M. W., Moss, D. S., and Thornton, J. M. (1993) PROCHECK: a program to check the stereochemical quality of protein structure coordinates, *J. Appl. Crystallogr. 26*, 283−291.
30. Schuettelkopf, A. W., and van Aalten, D. M. F. (2004) PRODRG—a tool for high-throughput crystallography of protein-ligand complexes, *Acta Crystallogr., Sect. D: Biol. Crystallogr. 60*, 1355−1363.
31. Hubbard, P. A., Yu, W., Sculz, H., and Kim, J.-J. P. (2005) Domain swapping in the low-similarity isomerase/hydratase superfamily: the crystal structure of rat mitochondrial Δ^3,Δ^2-enoyl-CoA isomerase, *Protein Sci. 14*, 1545−1555.
32. Tejero, J., Perez-Dorado, I., Maya, C., Julvez, M. M., Sanz-Aparicio, J., Gomez-Moreno, C., Hermoso, J. A., and Medina, M. (2005) C-terminal tyrosine of ferredoxin-$NADP^+$ reductase in hydride transfer processes with $NADP^+$/H, *Biochemistry 44*, 13477−13490.
33. Rao, P. V. L., Gupta, N., Bhaskar, A. S. B., and Jayaraj, R. (2002) Toxins and bioactive compounds from cyanobacteria and their implications on human health, *J. Environ. Biol. 23*, 215−224.
34. Juttner, F. (1995) Physiology and biochemistry of odorous compounds from fresh-water cyanobacteria and algae, *Water Sci. Technol. 31*, 69−78.
35. Gu, L., Jia, J., Liu, H., Håkansson, K., Gerwick, W. H., and Sherman, D. H. (2006) *J. Am. Chem. Soc. 128*, 9014−9015.

BI061900G